UC Irvine
UC Irvine Previously Published Works

Title
Integrase Mediates Nuclear Localization of Ty3

Permalink
https://escholarship.org/uc/item/4v59035b

Journal
Molecular and Cellular Biology, 21(22)

ISSN
0270-7306

Authors
Lin, Sophia S
Nymark-McMahon, M Henrietta
Yieh, Lynn
et al.

Publication Date
2001-11-01

DOI
10.1128/mcb.21.22.7826-7838.2001

Integrase Mediates Nuclear Localization of Ty3

SOPHIA S. LIN, M. HENRIETTA NYMARK-McMAHON, LYNN YIEH, AND SUZANNE B. SANDMEYER*

Department of Biological Chemistry, University of California, Irvine, California 92697

Retroviruses in nondividing cells and yeast retrotransposons must transit the nuclear membrane in order for integration to occur. Mutations in a bipartite basic motif in the carboxyl-terminal domain of the Ty3 integrase (IN) protein were previously shown to block transposition at a step subsequent to 3′-end processing of Ty3 extrachromosomal DNA. In this work, the Ty3 IN was shown to be sufficient to target green fluorescent protein to the nucleolus. Mutations in the bipartite basic motif abrogated this localization. The region containing the motif was shown to be sufficient for nuclear but not subnuclear localization of a heterologous protein. Viruslike particles (VLPs) from cells expressing a Ty3 element defective for nuclear localization were inactive in an in vitro integration assay, suggesting that nuclear entry is required to form active VLPs or that this motif is required for post-nuclear entry steps. Ty3 inserts at transcription initiation sites of genomic tRNA genes and plasmid-borne 5S and U6 RNA genes transcribed by RNA polymerase III. In situ hybridization with Ty3- and Ty3 long terminal repeat-specific probes showed that these elements which are associated with tRNA genes do not colocalize with the ribosomal DNA (rDNA). However, a PCR assay of cells undergoing transposition showed that Ty3 insertion does occur into the 5S genes, which, in yeast, are interspersed with the rDNA and therefore, like Ty3 IN, associated with the nucleolus.

The mechanisms used by viral complexes to enter the nucleus are diverse (50). Some retroviruses access the chromatin in mitotic cells, in which the nuclear membrane is not intact. Lentiviruses access the nucleus in nondividing cells, a process which is mediated by redundant functions (15). In contrast, all fungal retrotransposons are assumed to have mechanisms for nuclear entry of the preintegration complex, as the nuclear membrane does not break down, even during cell division. However, among the fungal elements which have been characterized, the nuclear localization signal (NLS) and its context are not conserved. Nuclear entry is presumed to be preceded by remodeling of the retroviral core or retrotransposon virus like particles (VLPs) to allow passage through the nuclear pore. This study was undertaken in order to elucidate the nuclear transport mechanism for Ty3, a gypsylike element in the yeast *Saccharomyces cerevisiae*.

Many nuclear proteins access the nuclear translocation machinery through interactions between a mono- or bipartite basic NLS and the NLS receptor importin α (reviewed in reference 12). The position of this domain in the primary sequence, as well as the contribution of flanking sequence to its function, is variable. Importin α associates with importin β, which interacts with members of the nuclear porin family. Subsequent to the original discovery of importin α and importin β, importin β-related proteins have been identified that mediate nuclear translocation of certain classes of proteins independent of importin α.

The lentiviruses infect nondividing cells, and their nuclear localization mechanisms have been studied extensively. Human immunodeficiency virus (HIV) nuclear localization is contributed to by functions of the matrix (MA), viral protein R (Vpr), and integrase (IN) (7, 15). Phosphorylated MA associates with IN and appears to facilitate its nuclear entry (16). Vpr, a small auxiliary protein was found to be required for infection of nondividing cells and thus implicated in nuclear translocation of the preintegration complex (24). Further in vitro studies have shown that the amino-terminal domain of the nuclear receptor importin α associates with the alpha-helical domain of Vpr (33). This importin α domain is separate from the domain that interacts with the conventional simian virus 40 (SV40) monopartite basic NLS.

Although Vpr bound to importin β appears to dock at nuclear pores by itself, as part of the preintegration complex, Vpr binding to nucleoporins is dependent on importin α (43). HIV-1 IN has a distinct, bipartite, basic NLS in its carboxyl-terminal region that has been shown to mediate nuclear localization of heterologous proteins, including green fluorescent protein (GFP) and β-galactosidase (16, 42). This domain may have additional functions, because mutations abrogate infection of dividing as well as nondividing cells (16). Aspects of chromatin access are also incompletely understood in the case of retroviruses believed to infect only dividing cells. For example, avian sarcoma virus (ASV) IN can mediate nuclear localization of heterologous domains, including GFP (30), and this activity appears to be attributable to a bipartite basic sequence. As for the HIV NLS, mutations in this domain block replication in dividing cells.

There is evidence that nuclear import is contingent on completion of specific stages of replication in at least some viruses, implying either that certain processes are required for exposure of the IN NLS or that there are additional signals. HIV mutations that disrupt replication at the internal plus strand start site inhibit the appearance of closed circles. Because the appearance of closed circular DNA is equated with exposure of the linear viral DNA to nuclear ligases, this suggests that nuclear entry requires initiation of plus-strand replication (55).

Retroviruslike elements are similar to retroviruses in that

* Corresponding author. Mailing address: Department of Biological Chemistry, College of Medicine, University of California, Irvine, Irvine, CA 92697-1700. Phone: (949) 824-7571. Fax: (949) 824-2688. E-mail: sbsandme@uci.edu.

they encode major structural and catalytic proteins in the upstream and downstream portions of their genomes, respectively, and replicate through reverse transcription of the genomic RNA (5, 44). Nuclear localization has been characterized for the copialike Ty1 elements from budding yeast and the gypsylike element Tf1 from fission yeast. In the case of the copialike elements, IN is encoded upstream of the coding region for reverse transcriptase (RT), while in the case of the gypsylike elements, it is encoded downstream, as it is for retroviruses. Nuclear entry in the case of the yeast copialike element Ty1 is dependent on a bipartite, basic NLS that has been mapped to the carboxyl-terminal domain of IN (27, 36). This domain has been shown to be competent to mediate nuclear localization of heterologous proteins, and mutations in this domain block transposition. Tf1 encodes its proteins in a single open reading frame (ORF) (1). In this gypsylike system, Gag contains a monopartite basic NLS (13).

The Ty3 gypsylike element contains separate *GAG3* and *POL3* ORFs. *POL3* encodes protease (PR), RT, and IN. The IN domain of Ty3 is found in VLPs as a 115-kDa fusion with RT and as processed 61- and 58-kDa forms (20, 29). Ty3 is unusual in that integration occurs exclusively at the sites of RNA polymerase III transcription initiation. Alignment of Ty3 IN with retroviral IN proteins shows that it contains a conserved central domain with residues important for catalysis of strand transfer and nonconserved amino- and carboxyl-terminal domains (22). In a previous study, alanines were substituted for charged residues in the nonconserved amino- and carboxyl-terminal domains in order to gain insight into their possible functions (39). Of the mutations that completely blocked transposition, two mutations were identified in the carboxyl-terminal domain of IN that appeared to act late in the Ty3 lifecycle. The resulting mutant elements were examined for particle formation, protein maturation, reverse transcriptase activity, DNA production, 3′-end processing, and transposition. Mutants that were active in 3′-end processing of the Ty3 DNA were presumed to have catalytically active IN. Two of these mutants, 412A(2) with mutations E412A, D414A, and 419A(3), with KKK (amino acids [aa] 419 to 421) changed to AAA, were normal for 3′-end processing but completely defective for transposition (39). These mutations did not affect particle assembly or protein processing, reverse transcription, or 3′ processing activity.

We report here that Ty3 IN mediates localization of a heterologous protein to a subnuclear compartment. Similar to Ty1 but different from Tf1, nuclear localization activity is associated with a carboxyl-terminal basic, bipartite NLS. Mutations in this domain block nuclear localization of Ty3 and in vitro integration mediated by Ty3 VLPs.

MATERIALS AND METHODS

Strains and culture conditions. *Escherichia coli* and *S. cerevisiae* strains were cultured and transformed by standard methods (2) except as otherwise indicated. The *S. cerevisiae* strains used in this study are W303-1a (NOY505) (41), kindly provided by M. Nomura (University of California [UC] Irvine); NOY770, an *rdn*ΔΔ derivative of NOY505 (41); and yTM443, a derivative of yVB110 which contains no endogenous copies of Ty3 (4, 35) (Table 1). Yeast transformations were performed by the lithium acetate procedure or the dimethyl sulfoxide (DMSO) method (46). Rich medium for *S. cerevisiae* cultures was YPD (1% yeast extract, 2% peptone, 2% dextrose). When selection was necessary, synthetic 2medium was used that contained dextrose (SD) (0.67% yeast nitrogen

base, 2% dextrose), galactose (SG) (0.67% yeast nitrogen base, 2% galactose), or raffinose as a carbon source (SR) (0.67% yeast nitrogen base, 2% raffinose) and lacked only the specified essential amino acids. *E. coli* RZ1032 [*lysA*(61–62) *thi-1 relA1 spoT1 dut-1 ung-1* (Tet^r) *supE44*] was used for production of single-stranded DNA for site-directed mutagenesis (31). Plasmids were amplified in HB101 (F$^-$ *hsd-20* [r_B^- m_B^-] *recA13 leuB6 ara-14 proA2 lacY1 galK2 rpsL20* [Sm^r] *xyl-5 mtl-1 supE44* λ$^-$).

Plasmids. Recombinant DNA techniques were performed essentially as described in *Current Protocols in Molecular Biology* (2). Ty3 elements modified by replacement of the regulatory region with sequences from the *GAL1* upstream activation sequence (UAS$_{GAL1}$), were used for transposition studies and for preparation of whole-cell extracts. The wild-type Ty3 was expressed from plasmid pEGTy3-1 (21). The catalytic site mutant IN(D255E/E261D) (29) was expressed from plasmid pJK784. The pEGTy3-1 and pJK784 plasmids contain the 2μm sequence for maintenance at high copy number in *S. cerevisiae* and the yeast selectable marker *URA3*, which allows cells containing this plasmid to be selected by growth on medium lacking uracil. The target plasmid used in the transposition assays, pCH2bo19V (28), contains the *ARS1* and *CEN4* sequence for maintenance at low copy number in *S. cerevisiae* and the yeast selectable marker *HIS3*.

IN was expressed in yeast under control of the *GAL1* promoter (P$_{GAL1}$) in plasmid pJK788 (J. Kirchner, unpublished data). PJK788 was constructed from sequences of a Ty3-1 subclone in pVB193 (4).

PVB193 was mutagenized to make pJK802, using site-specific oligonucleotide mutagenesis (31). Oligonucleotides used for mutagenesis and in PCR are described in Table 2. An *Eco*RI site and an ATG start codon were inserted just upstream of the IN coding region. The *Eco*RI/*Xho*I fragment containing the IN coding region was then inserted into pYES2.0 (Invitrogen, Carlsbad, Calif.), creating pJK788. The IN coding region was then modified to encode a catalytic site mutant (D255E/E261D) using site-directed mutagenesis (31).

To make IN–green fluorescent protein (GFP) fusions, a *Bam*HI site was substituted for the IN stop codon in pJK802 using oligonucleotide 474. The coding region for S65T GFP was isolated on a *Bam*HI fragment from pRSET-GFP (gift from R. Tsien, UC San Diego) and inserted in frame downstream of the IN coding region. The plasmid was digested completely with *Xho*I and partially with *Eco*RI, yielding an *Eco*RI/*Xho*I fragment containing the IN-GFP coding region. This fragment was inserted into pYES2.0 to yield pSSL1648. IN-GFP mutants were created by mutagenizing the IN coding sequence in pJK802 and subcloning the *Eco*RI/*Xho*I fragment carrying the IN coding region into pYES2.0. The *Hin*dIII-*Mlu*I fragment containing the mutations was finally exchanged with the analogous fragment in pSSL1648 to generate a series of clones expressing the various IN-GFP mutants.

The candidate NLS domains were expressed in frame with the fused coding regions for S65T GFP (23) and enhanced GFP (eGFP) (2×GFP). In order to construct the fusion, the coding region for S65T GFP was subcloned into pYES2.0 on a *Bam*HI fragment to yield pYES-GFP. A *Bgl*II site replacing the GFP stop codon was created in this clone using oligonucleotide 569. The *Bam*HI fragment containing the eGFP coding region (Clontech Laboratories Inc.) was then joined in frame at this *Bgl*II site to create pSSL2010. The sequences encoding the candidate NLS peptides were amplified by PCR using primers with *Sac*I sites, digested with *Sac*I, and ligated into pSSL2010, creating pSSL2009. PSSL2009 was then mutagenized using oligonucleotides (587 to 590 and 611 to 614) to generate N-terminal and C-terminal deletion mutants. Peptide domains are referred to by the first and last IN codons present in the fusion construct.

In order to monitor transposition in vivo, Ty3 expression plasmid pMA1833 and its derivative pMA1890(SSL) were used. Plasmid pMA1833 (M. Aye, personal communication) contains the *URA3* marker, *ARS1/CEN4*, and a galactose-inducible Ty3-1 element. The negative control, pMA1890(SSL), is a D224E/E261D derivative of pMA1833 but contains a *TRP1* marker in addition to *URA3*. A plasmid, pDLC301 (10), containing a copy of the 5S rDNA gene, 2μm sequence, and *HIS3* was used as a negative control for PCR. PDLC322, containing a Ty3 insertion upstream of the 5S rDNA gene in pDLC301 (D. Chalker, unpublished data), was used as a positive control.

The GFP fusion vectors pNfus-GFP and pGFP-NOP8 (54) were used as negative and positive markers for nucleolar localization, respectively (both were generous gifts from D. Goldfarb, University of Rochester). To express IN-GFP under the control of the *MET25* promoter (P$_{MET25}$) (37), GFP-*NOP8* on a *Hin*dIII/*Xho*I fragment was substituted with the *Hin*dIII/*Xho*I fragment carrying IN-GFP from pSSL1648.

Localization of wild-type and catalytic site mutant IN-GFP fusions was tested in a background in which the nucleoli were disrupted (NOY770) (40). In this experiment, the fusions were expressed from a low-copy-number plasmid. The region containing the cloning site of pYES2.0 together with its promoter and terminator sequences was amplified from template pYES2.0 in a PCR primed

TABLE 1. Strains and plasmids used in this study

Strain or plasmid	Relevant markers	Reference
Strain		
W303-1a	*MAT***a** *ade2-1 ura3-1 leu2-3,112 his3-11 trp1-1 can1-100*	41
NOY770	*MAT***a** *ade2-1 ura3-1 leu2-3,112 his3-11 trp1-1 can1-100 rdn1ΔΔ::HIS3 pRDN-hyg1*	40
yTM443	*MAT***a** *trp1-H3 ura3-52 his3-Δ200 ade2-101 lys2-1 leu1-12 can1-100 ΔTy3 bar1::hisG GAL3$^+$*	35
Plasmids		
pDLC301	2μm *amp^r*, *URA3*, 5S rDNA	10
pDLC322	2μm *amp^r*, *URA3*, Ty3::5S rDNA	D. Chalker, unpublished data
pHN1743	2μm *amp^r* *URA3* UAS$_{GAL1}$-Ty3[IN 404A(2)]	39
pHN1744	2μm *amp^r* *URA3* UAS$_{GAL1}$-Ty3[IN 412A(2)]	39
pHN1745	2μm *amp^r* *URA3* UAS$_{GAL1}$-Ty3[IN 419A(3)]	39
pJK784	2μm *amp^r* *URA3* UAS$_{GAL1}$-Ty3, IN(D255E/E261D)	29
pJK788	2μm *amp^r* *URA3* P$_{GAL1}$-IN	29
pJK802	*amp^r* pVB193 with *Eco*RI site and ATG 5′ of Ty3 IN	J. Kirchner, unpublished data
pLY1855	pU6LboxB ΔδTATA box	63
pMA1833	*ARS4/CEN6 amp^r URA3* UAS$_{GAL1}$-Ty3	M. Aye, unpublished data
pMA1890	*ARS4/CEN6 amp^r URA3* UAS$_{GAL1}$-Ty3, IN(D255E/E261D)	M. Aye, unpublished data
pSSL1649	2μm *amp^r* *URA3* P$_{GAL1}$-IN-GFP D255E/E261D	This work
pSSL1650	2μm *amp^r* *URA3* P$_{GAL1}$-IN-GFP K419A(3)	This work
pSSL1654	2μm *amp^r* *URA3* P$_{GAL1}$-IN-GFP 404A(2)/412A(2)/419A(3)	This work
pSSL1655	2μm *amp^r* *URA3* P$_{GAL1}$-IN-GFP 404A(2)	This work
pSSL1656	2μm *amp^r* *URA3* P$_{GAL1}$-IN-GFP 412A(2)	This work
pSSL1677	2μm *amp^r* *URA3* P$_{GAL1}$-SV40 T-antigen NLS-GAL4 active domain-GFP	This work
pSSL2010	2μm *amp^r* *URA3* P$_{GAL1}$-2×GFP	This work
pSSL2009	2μm *amp^r* *URA3* P$_{GAL1}$-395-439 IN-2×GFP	This work
pSSL2021	2μm *amp^r* *URA3* P$_{GAL1}$-401-439 IN-2×GFP, oligo 587	This work
pSSL2023	2μm *amp^r* *URA3* P$_{GAL1}$-395-432 IN-2×GFP, oligo 589	This work
pSSL2025	2μm *amp^r* *URA3* P$_{GAL1}$-401-432 IN-2×GFP, oligos 587/589	This work
pSSL2034	2μm *amp^r* *URA3* P$_{GAL1}$-403-439 IN-2×GFP, oligo 611	This work
pSSL2035	2μm *amp^r* *URA3* P$_{GAL1}$-395-436 IN-2×GFP, oligo 612	This work
pSSL2036	2μm *amp^r* *URA3* P$_{GAL1}$-395-436 IN-2×GFP, oligo 613	This work
pSSL2037	2μm *amp^r* *URA3* P$_{GAL1}$-395-436 IN-2×GFP, oligo 614	This work
pSSL2040	2μm *amp^r* *URA3* P$_{GAL1}$-395-436 IN-2×GFP, oligos 587/614	This work
pSSL2041	2μm *amp^r* *URA3* P$_{GAL1}$-395-436 IN-2×GFP, oligos 587/612	This work
pSSL2042	2μm *amp^r* *URA3* P$_{GAL1}$-395-436 IN-2×GFP, oligos 587/613	This work
pSSL2047	*ARS4/CEN6 amp^r TRP1*, P$_{GAL1}$-MCS-t$_{CYC1}$	This work
pSSL2050	*ARS4/CEN6 amp^r TRP1*, P$_{GAL1}$-IN	This work
pSSL2051	*ARS4/CEN6 amp^r TRP1*, P$_{GAL1}$-IN D255E/E261D	This work
pSSL2061	2μm *amp^r* *URA3* P$_{MET25}$-IN-GFP	This work
pVB193	*amp^r* Ty3-1 *Sal*I-*Eco*RI fragment in pIBI20	V. Bilanchone, unpublished data
pBR328	*amp^r*	Boehringer Mannheim Corp
pCH2bo19v	*ARS1/CEN4 amp^r HIS3* tDNA^{Val}-sup2o Ty3 integration target	28
pEGTY3-1	2μm *amp^r* *URA3* UAS$_{GAL1}$-Ty3	21
pGFP-NOP8	2μm *amp^r* *URA3* P$_{MET25}$-GFP-*NOP8*	54
pNfus-GFP	2μm *amp^r* *URA3* P$_{MET25}$-GFP	54
pRDN-hyg1	2μm *amp^r* *rdn-hyg1 rdn-ani1 leu2-d URA3*	11
pYES2.0	2μm *amp^r* *URA3* P$_{GAL1}$	Invitrogen

with oligonucleotides 807 and 808 (Table 2). This fragment was restricted with *Sma*I and ligated to pRS314 (48) linearized with *Pvu*II, yielding pSSL2047. PSSL2047 was restricted with *Sst*I and *Xho*I. The *Sst*I/*Xho*I fragments encoding the wild-type IN-GFP from pSSL1648 and the catalytic site mutant IN-GFP from pSSL1649 were ligated to linearized pSSL2047 to yield pSSL2050 and pSSL2051, respectively.

In vitro integration into *SNR6* targets. In vitro integration reactions were performed essentially as described (53). Briefly, samples for in vitro integration contained, in 50 μl of reaction buffer (40 mM Tris-HCl [pH 8.0,] 7 mM MgCl$_2$, 3 mM dithiothreitol [DTT], 100 μg of bovine serum albumin [BSA] per ml, and 50 mM NaCl), recombinant TFIIIB (50 fmol of TATA-binding protein, 36 fmol of Brf, and 75 fmol of B″) and 178 fmol of *SNR6* target plasmid pLY1855 DNA. Recombinant TFIIIB was a gift from G. Kassavetis and E. P. Geiduschek (UC San Diego). These components were incubated for 30 min at 23°C and shifted to 15°C, and 5 μg of Ty3 VLP protein was added, followed by incubation at 15°C for 15 min. Reactions were stopped by adding proteinase K, sodium dodecyl sulfate (SDS), and EDTA (pH 8.0) to final concentrations of 0.2 mg/ml, 0.2% (wt/vol), and 20 mM, respectively, and incubating at 37°C for 30 min. Reaction products were extracted with phenol-chloroform, and DNA was precipitated and redissolved in 10 mM Tris-HCl (pH 8.0)–1 mM EDTA.

PCR was performed essentially as described (53), using primers 242 and 411 to amplify portions of Ty3 integrations in the target plasmid and primers 679 and 680 to amplify the β-lactamase gene on the target plasmid to monitor DNA

recovery. PCR products were resolved by electrophoresis on nondenaturing 8% polyacrylamide gels and visualized by staining with ethidium bromide.

Fluorescence microscopy. Transformants of cells containing the IN-GFP constructs, pSSL1648, -1649, -1650, -1654, and -1655, -1656, were inoculated in SR-Ura medium containing 1.25 μg of 4′,6-diamidino-2-phenylindole (DAPI) and grown at 30°C to early log phase (optical density at 600 nm [OD$_{600}$] of 0.1 to 0.3). Protein expression was induced by adding galactose to 2% final concentration, followed by incubation for 30 min. Glucose was then added to 2% final concentration, and the incubation was continued for 1 h to repress galactose-induced expression. The cells were pelleted, washed once, and resuspended in SR-Ura. Cells were applied to microscope slides and visualized with a Zeiss Axioplan 2 (Carl Zeiss Inc., Oberkochen, Germany) fluorescence microscope equipped with a SenSys camera (Photometrics, Tucson, Ariz.) with a 100× objective using filters for fluorescein, rhodamine, and UV detection. Digital images were collected using the Kontran Software 400 (Carl Zeiss Inc.) or Axiovision 2. Images were processed, pseudocolored, and superimposed for composites using Adobe Photoshop 5.0 (Adobe Systems Inc.). Transformants containing the various deletion NLS-2XGFP constructs (pSSL1677, -2010, -2009, -2021, -2023, -2025, -2034, -2035, -2036, -2037, -2040, -2041, and -2042) were similarly induced, visualized, and imaged.

For visualization of IN-GFP under control of the P$_{MET25}$, single-colony transformants of cells were inoculated under conditions of constitutive expression in SD-Ura-Met containing DAP1 (1.25 μg/ml) and grown overnight at 30°C. The

TABLE 2. Oligonucleotides[a]

Name (strand)	Sequence (5′ to 3′)	Related construct
263 (−)	GACATCTCTTTCACTGGTTA	IN D224E
264 (−)	GTATCGTTCGATCGGATTGTC	IN E261D
372 (−)	GTTATCGTTTATTGCCGCGACAACTCG	IN 404A(2)
373 (−)	GAGAGTTTAAAGCTAGTGCGTAGGCGTTATC	IN 412A(2)
374 (−)	CTCTGTGCGCTGCCGCGTGAGAG	IN 419A(3)
411 (+)	CGAAACACAAGACAACCC	Ty3 4979-4996 amplify IN
242 (−)	GGAACTGCTGATCATCTCT	Amplify $SNR6$ inserts
679 (+)	ACTCCCGTCGTGTAGATAACTACG	Amplify Amp^r
680 (−)	AAGCCATACCAAACGACGAGC	Amplify Amp^r
499 (+)	AGGAGCTCAAATGTACGTCGGACC	Add SacI, amplify IN NLS
500 (−)	TTGAGCTCGCGTCTGGACGGTATAC	Add SacI, amplify IN NLS
547 (−)	CAGCGGGGGAGATCTTATCG	Add BglII to replace BamHI at N-terminal of GFP
551 (+)	CCGAGCTCAAATGAAGAAAATAAACGATAACGCC	NLS-GFP (K$_{404}$KINDNAY-)
587 (+)	CGAGCTCAAATGCGAGTTGTCAAG	NLS-GFP (R$_{401}$VVK-)
589 (+)	CCTGAAAAAGATGAGTAAAGGAG	NLS-GFP (-LKK$_{432}$)
611 (+)	CGAGCTCAAATGGTCAAGAAAATAAACG	NLS-GFP (V$_{403}$KKIN-)
612 (+)	GTATACCGTATGAGTAAAGGAG	NLS-GFP (-VYR$_{436}$)
613 (+)	CCGTCCAGACATGAGTAAAGGAG	NLS-GFP (-RPD$_{438}$)
614 (+)	GTACAATTCCTGATGAGTAAAGGAG	NLS-GFP (-VQFL$_{430}$)
719 (+)	TCCGTTAAACTATCGGTTGCGGCC	Overlap 5S rDNA transcription start
720 (+)	GCACCTGAGTTTCGCGTATGGTC	Overlap 5S rDNA transcription termination site
721 (+)	GGTTGCGGCCATATCTACCAGAAAGC	Overlap 5S rDNA transcription start
807 (+)	GATCCCCGGGTACGGATTAGAAGC	Add SmaI, amplify P$_{GAL1}$-MCS-t$_{CYC1}$ from pYES2.0
808 (−)	CGTTGCCCGGGGTTCATTAATGCAGG	Add SmaI, amplify P$_{GAL1}$-MCS-t$_{CYC1}$ from pYES2.0

[a] Mutated residues are underlined.

cells were diluted and grown to early log phase (OD$_{600}$ of 0.1 to 0.3), pelleted, washed, and resuspended in SD-Ura-Met. Cells were mounted onto microscope slides and visualized as described above. For visualization of IN-GFP in the $rDNA$ deletion strain NOY770, single-colony transformants containing plasmid pSSL2050 or pSSL2051 were induced and processed as described for IN-GFP.

Immunofluorescence microscopy. Immunofluorescence microscopy was carried out essentially as described (41). Yeast cells transformed with IN-expressing construct pJK788 or pSSL1639 or pYES2.0 as a negative control were isolated as single colonies in SD-Ura and grown at 30°C overnight in SR-Ura to early log phase (OD$_{600}$ of 0.1 to 0.2). Galactose was added to 2% final concentration, and cells were incubated for 3 h at 30°C. For visualization of IN and nucleolar proteins, cells were first fixed in 3.7% formaldehyde for 10 min, digested with Zymolase 100T (Seikagaku Corp.) and glucuronidase (Sigma, St. Louis, Mo.), applied to polylysine-coated slides, and permeabilized with methanol followed by acetone. The immunoglobulin G (IgG) fraction of rabbit anti-IN antiserum was affinity purified over an IN-Sepharose column and used at a 1:1,000 dilution in phosphate-buffered saline (PBS) containing BSA (1 mg/ml). The IgG fraction was preadsorbed on fixed cells to reduce nonspecific binding. Mouse YN2C1 serum (a gift from M. Nomura, UC. Irvine), containing antinucleolar protein antibody, was used at a 1:1,000 dilution in PBS-BSA. Rabbit IgG was detected with fluorescein isothiocyanate (FITC)-conjugated or Alexa-488 (Molecular Probes)-conjugated anti-rabbit IgG (Sigma) in PBS-BSA at a 1:2,000 dilution. Mouse IgG was detected with tetramethyl rhodamine isocyanate (TRITC)-conjugated or Alexa-586-conjugated goat anti-mouse IgG (Sigma) in PBS-BSA at a 1:2,000 dilution. The mounting medium (90% glycerol and DAPI at 1 μg/ml [Sigma] was used to stain DNA.

FISH. Fluorescent in situ hybridization (FISH) was performed as described (8, 19). Plasmid pRDN-hyg1 (11) was digested with BamHI, and the rDNA-containing fragment was isolated and biotinylated using the Random Prime labeling system (Boehringer Mannheim Corp., Indianapolis, Ind.) to detect rDNA. The control plasmid pBR328 was digested with EcoRI and labeled with digoxigenin using the Random Prime labeling system containing digoxigenin-11-UTP (Boehringer Mannheim Corp.). The XhoI fragment of pEGTy3 was similarly labeled with digoxigenin. The long terminal repeat (LTR) sequence was amplified in the presence of digoxigenin-11-UTP using primers 562 and 563. Hybridized biotinylated probes were detected by successive incubations in FITC-avidin (5 μg/ml), biotinylated antiavidin (5 μg/ml), and finally FITC-avidin (5 μg/ml). Hybridized digoxigenin probes were detected using mouse antidigoxigenin at a 1:250 dilution (Boehringer Mannheim Corp.) and then anti-mouse Alexa 586 (Molecular Probes, Eugene, Oreg.) at a 1:1000 dilution. FISH was performed using the microscope, camera, and software described above.

In vivo integration and PCR detection of transposition into genomic 5S rDNA targets. Yeast cells transformed with pMA1833 or pMA1890, the low-copy-number plasmids expressing wild-type or catalytic site mutant IN-GFP, were isolated on SD-Ura. Cells were grown at 30°C to log phase (OD$_{600}$ of 0.3 to 0.4). Ty3 transcription was induced for 6, 9, or 18 h by adding galactose to 2% final concentration. The cells were harvested, and DNA was extracted. PCR was performed as described previously (35) except that primers 411 and 729 were used, which annealed in the Ty3 element and in the 5S rDNA gene, respectively, to allow amplification of insertions in the rDNA repeat. The 125 ng of genomic DNA was incubated for 2.5 min at 95°C, followed by 40 cycles of denaturation at 94°C for 1 min, renaturation at 60°C for 30 s, and extension at 72°C for 30 s. PCR products were resolved by electrophoresis on nondenaturing 8% polyacrylamide gel and visualized by staining with ethidium bromide. The gel image was photographed using a digital camera, and PCR products were quantified by NIH image.

RESULTS

Ectopically expressed Ty3 IN localizes to the yeast nucleus. In a previous study, alanine scanning mutations were introduced throughout the nonconserved amino-terminal and carboxyl-terminal domains of Ty3 IN (39). Two mutants, 412A(2) and 419A(3), produced wild-type patterns of Ty3 DNA, including 3′-end processing (39). Mutated residues in these elements were within a region containing a concentration of basic amino acids, prompting analysis of IN for an NLS. Gag3p and Pol3p predicted protein sequences were subjected to analysis using PSORT (http://psort.nibb.ac.jp/), a protein-sorting signal prediction program (38). Within the IN sequence, two potential NLS motifs were identified, Q$_{363}$RRKP and K$_{419}$KKHR. Inspection of the region containing residue 419 showed that basic residues also occurred amino-terminal to KKKHR, at positions 404 and 405. A new mutant was constructed in which these two residues were changed to alanine [mutant 404A(2)]. This mutant was shown to have normal levels of correctly processed IN and cDNA but to be moderately reduced for
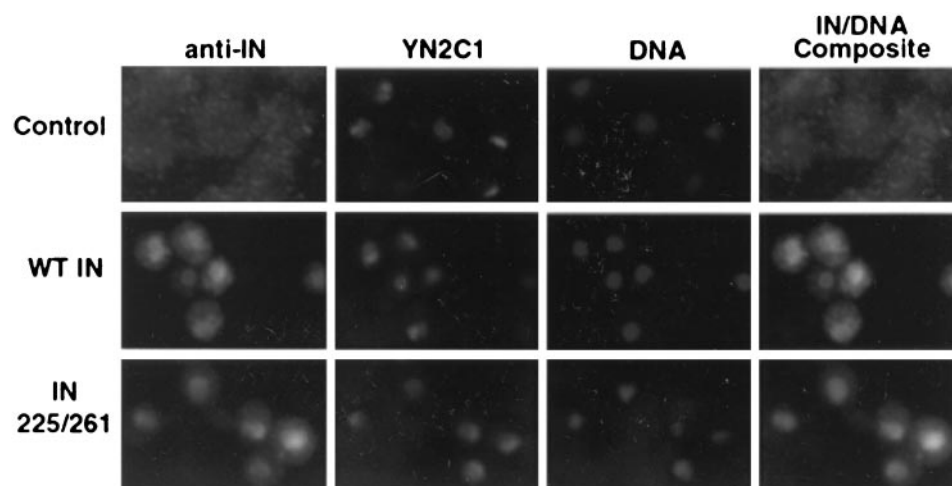
FIG. 1. Nuclear localization of Ty3 IN and nucleolar antigen using double indirect fluorescence microscopy. Yeast cells expressing Ty3 wild-type (WT) and D255E/E261D mutant IN induced under P_{GAL1} were analyzed for the localization of Ty3 IN using anti-IN rabbit IgG (Alexa-488) and nucleolar proteins using mouse antiserum YN2C1 (Alexa-586). Images were recorded on an automatic exposure setting, which resulted in longer exposure of control cells. DNA was visualized using DAPI.

transposition (data not shown). The domain from aa 404 to 421 has basic residues at each end and several acidic residues in the intervening region. Thus, it loosely resembles the bipartite type of NLS observed in the carboxyl-terminal domain of Ty1 (27, 36) and HIV IN proteins (16).

The observation that mutations in a basic region in the carboxyl-terminal domain of IN interfered with a late step in the Ty3 life cycle suggested that the mutated region contained the Ty3 NLS. We first tested this hypothesis by examining whether IN, if expressed in the absence of other Ty3 proteins, localized to the nucleus. Yeast strain W303-1a transformed with the vector alone or with a plasmid producing wild-type Ty3 IN (pJK788) or IN(D255E/E261D) (pSSL1639) was grown in galactose-containing medium. IN(D225E/E261D) is a catalytic site mutant which produces IN and synthesizes cDNA (39). It was used as a control throughout this study in order to detect any effects attributable to the expression of a strand transferase that was not associated with a VLP. Transformants were cultured in the presence of DAP1 for 10 to 12 h and induced for 30 min, followed by 1 h of incubation in glucose-containing medium. They were prepared and visualized by fluorescence microscopy as described in Materials and Methods (Fig. 1). Overlay of the IN and DAPI images showed that staining of wild-type and mutant IN was concentrated within the nucleus, but that IN was not distributed throughout the nucleus.

Ty3 IN-GFP fusion protein localizes to the nucleus, and mutations in bipartite basic region disrupt this localization. Because processing cells for indirect immunofluorescence can disrupt nuclear organization, fusions of IN to GFP (23) were used to localize Ty3 IN in living cells. In addition, these constructs could be used together with fusions involving smaller domains to delimit the IN NLS. Plasmids expressing wild-type IN-GFP (pSSL1648) and catalytic site mutant (D255E/E261D) IN-GFP (pSSL1649) were used to visualize IN localization (Fig. 2A). In order to limit GFP diffusion into the nucleus, a construct was also created in which GFP coding sequence was

tandemly repeated (pSSL2010). For a positive control, the SV40 large T antigen (LgTAg) NLS (26) was fused to the tandemly repeated GFP (pSSL1677). These plasmids were transformed independently into yeast strain W303-1a. Transformants were cultured and induced as described above and in Materials and Methods.

Cells expressing the tandem GFP repeat protein (2×GFP) showed bright fluorescence throughout the cell except for the vacuole (Fig. 2B). Apparent nuclear staining may have occurred due to partial degradation of the tandem GFP and diffusion into the nucleus or to weak NLS activity in GFP. The positive control cells, expressing the SV40 LgTAg NLS fused to GFP, showed very defined concentrations of GFP fluorescence overlapping the same region as DAPI staining (Fig. 2B). Cells expressing wild-type IN-GFP fusions showed a concentration of GFP fluorescence closely associated with or partially overlapping the DAPI staining (Fig. 2C). A similar pattern was observed for the catalytic site mutant IN-GFP (IN-GFP 225/261). Thus, Ty3 IN contains sequences capable of localizing a heterologous protein to the nucleus.

In order to test the hypothesis that mutations 404(2), 412A(2), and 419A(3) act by disrupting nuclear localization of IN, constructs in which these mutant domains were substituted for the wild-type Ty3 IN in pSSL1648 (Table 2) were transformed into yeast strain W303-1a. Cells were induced as described above. IN-GFP 404(2) localized to the nucleus but showed more cytoplasmic staining than wild-type IN-GFP. IN-GFP 412A(2) was slightly more diffuse than IN-GFP 404(2). IN-GFP 419A(3) showed the most diffuse fluorescence. Immunoblot analysis of wild-type and NLS mutant proteins showed that comparable amounts of the fusion proteins were present in cells, so that enhanced cytoplasmic staining was unlikely to arise from different amounts of free GFP (data not shown). The staining pattern of the triple mutant was comparable to the pattern of IN-GFP 419A(3). These results suggested that the region from aa 404 to 419 contributed to wild-type nuclear localization of IN, but that residues in the vicinity of 419
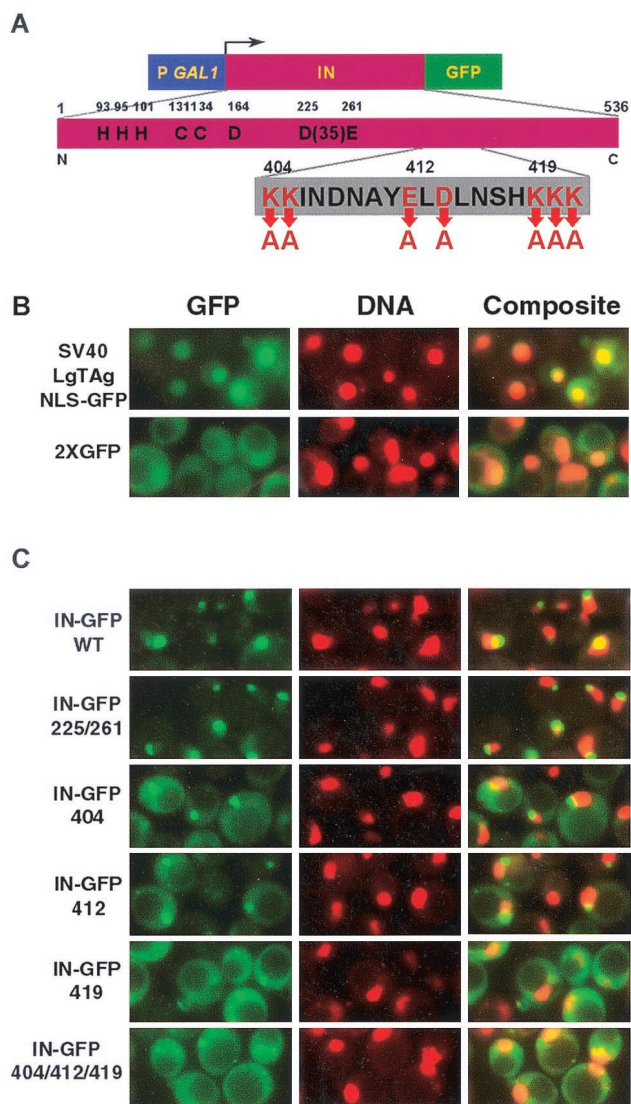
FIG. 2. Localization of Ty3 IN-GFP. (A) Wild-type (WT) IN-GFP and mutant IN-GFP constructs. Top, P$_{GAL1}$ followed by IN and GFP coding regions. Middle, expanded view of IN showing residues conserved among retrovirus IN proteins. Bottom, expanded view of Ty3 NLS. (B) Direct fluorescence microscopy of SV40 LgTAg NLS fused to GFP and 2×GFP. DNA was visualized with DAPI. Images of GFP and DNA were pseudocolored green and red, respectively. Individual images were overlaid, and regions of colocalization appear as orange to yellow fluorescence. (C) Direct fluorescence microscopy analysis of IN-GFP fusion protein localization. Yeast cells expressing wild-type Ty3 IN, D225E/E261D IN, 404(2) IN, 412A(2) IN, and 419A(3) IN fused to GFP were analyzed for fusion protein and DNA localization. Images were manipulated panel as in B.

contributed more significantly to localization than did residues clustered between aa 404 and 414. Thus, Ty3 IN can target a heterologous protein to the nucleus and has sequences in the region from aa 404 to 419 which contribute directly or indirectly to this localization.

A basic, bipartite motif in carboxyl-terminal domain of Ty3 IN is sufficient to mediate nuclear localization of a heterologous protein. Although the experiments described above showed that basic residues included in a potential NLS con-

tributed to nuclear localization, they did not show that this effect was direct or define the domain sufficient to confer nuclear localization. PCR was used to amplify the region encoding aa 396 to 439, including the putative NLS and flanking residues. Subdomains were also amplified using the appropriate primers. The products were cloned in frame with 2×GFP under control of P$_{GAL1}$ as described in Materials and Methods. These constructs were transformed into yeast and induced for GFP expression as described for IN-GFP. The aa 396 to 439 domain of Ty3 IN conferred nuclear localization on the fusion protein (Fig. 3A), similar to the the SV40 LgTAg NLS, indicating that it contained sequences sufficient for nuclear localization. In contrast to the pattern of IN-GFP staining, the peptide domain-GFP fluorescence occurred throughout the DAPI-stained region.

In order to define the limits of the domain both necessary and sufficient for nuclear localization of GFP, the IN aa 396 to 439 sequence was truncated at each end in different constructs and at both ends in the same construct. A domain from aa 401 to 439 did not have localization properties appreciably different from those of the domain from aa 396 to 439. In contrast, aa 403 to 439 did not confer nuclear localization (Fig. 3A), indicating that the amino terminus of the NLS lay between aa 401 and 403.

In order to define the carboxyl-terminal border of the NLS, successive deletions were introduced at the distal end of the aa 396 to 439 construct. The effect of deletions on this end was complex (Fig. 3B). Deletion of a single residue (construct aa 396–438) was sufficient to result in diffuse fluorescence (Fig. 3B). However, aa 396–436, aa 396–432, and aa 396–430 gave levels of nuclear localization comparable to that with aa 396–439. Although nuclear localization activity was associated with aa 396 to 430, at least a portion of the region from aa 430 to 439 appeared to have a negative effect, because the aa 396–438–2×GFP fusion was only weakly localized. The fusion peptide including aa 396 to 421 was cytoplasmic, with no observable nuclear localization (data not shown).

In order to define the region sufficient for localization of GFP to the nucleus, several combinations of carboxyl-terminal truncations were tested with the construct that had an amino-terminal IN residue at position 401, the most extreme of the amino-terminal deletions that still showed nuclear localization (Fig. 3C). In this context, nuclear localization was observed for 401–436, but fluorescence for the slightly longer construct 401–438 was more diffuse. Localization was weaker for 401–432 and was not observable for 401–430. These results were consistent with the weak localization observed for 396–438 and with the interpretation that residues at the carboxyl-terminal region might be slightly inhibitory. The most robust nuclear localization mediated by this region of Ty3 IN therefore corresponded to the region spanning aa 401 to 439. The sequence of this region is compared to the sequences of known NLS, including those for HIV-1 IN (16) and Ty1 IN (27, 36), in Table 3. As noted above, the NLS domain confers localization to the nucleus, but does not confer localization to the subcompartment, as observed for the IN-GFP fusions.

Mutations in Ty3 NLS block in vitro integration. The Ty3 element containing mutation 419A(3), which had the most dramatic effect on nuclear localization of Ty3 IN-GFP, was blocked at a late stage in integration. It is possible that Ty3
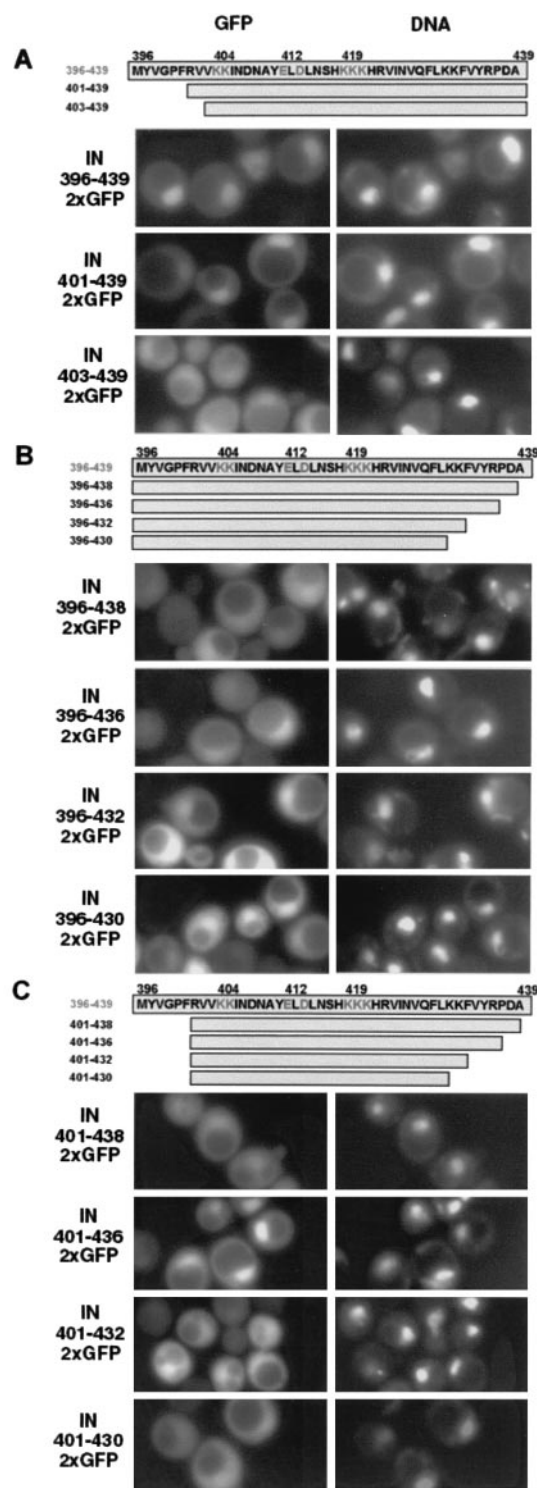
FIG. 3. Direct fluorescence analysis of IN peptide-2×GFP fusion protein localization. (A) Expression of amino-terminal deletion series of IN peptide domains fused to 2×GFP. Yeast cells expressing the indicated IN peptides fused to 2×GFP were analyzed for fusion protein and DNA localization as described in Materials and Methods and in the legend to Fig. 2 except that images are not shown in pseudocolor and overlay is omitted. (B) Expression of carboxyl-terminal deletion series of IN peptide domains fused to 2×GFP. Yeast cells expressing the constructs as described for panel A. (C) Expression of amino- and carboxyl-terminal IN peptide domains fused to 2×GFP. Yeast cells expressing the fusion constructs as described for panel A.

TABLE 3. Comparison of retroelement NLS[a]

Retro-element	NLS motif	Reference(s)
ASV IN	KTPIQKHWRPTVLTEGPPVKIRIETGEWEK	30
HIV-1 IN	KRKGGIGGYSAGERIVDIIATDIQTKELQK YITK	16
Ty1 IN	KKRSLEDNETEIKVSRDTWNTKNMRSLEP PRSKKR	36,27
Tf1-Gag	KKIR	13
Ty3 IN	R_{401}VVK$_{404}$KINDNAYE$_{412}$LDLNSHK$_{419}$KKH RVINVQFLKKFVYRPDA$_{439}$	This work

[a] Residues 404, 412, and 419 shown to be essential for wild-type levels of Ty3 transposition are indicated.

replication and uncoating are complete at the time of nuclear entry and the VLP fraction itself would therefore contain pre-integration complexes competent for integration. An in vitro assay for Ty3 integration into the U6 RNA gene (*SNR6*) (53) was used to determine the integration activity of the Ty3 VLP fraction from cells expressing the 419A(3) NLS mutant. This assay relies on amplification of a diagnostic Ty3-*SNR6* chimeric fragment from a plasmid-borne *SNR6* gene that has undergone Ty3 integration (Fig. 4).

Ty3 VLPs were prepared (20) from cells expressing wild-type and 419A(3) NLS mutant Ty3 elements from high-copy-
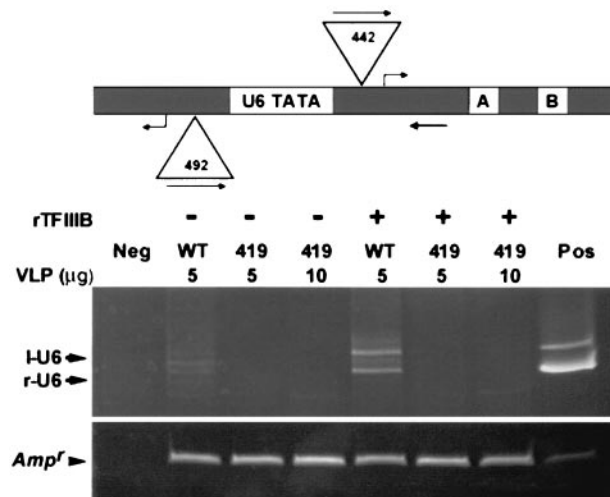

FIG. 4. In vitro integration into *SNR6* targets. Top, schematic of *SNR6* TATA flanked by two sites (left and right) for transcription initiation and Ty3 integration. Triangles indicate Ty3 insertion positions. Straight arrows show orientation and position of Ty3 and *SNR6* primers. Bent arrows show positions of transcription initiation. Samples for in vitro integration containing recombinant TFIIIB (rTFIIIB) and DNA were incubated for 30 min at 23°C and shifted to 15°C, and then 5 or 10 μg of protein of Ty3 wild-type (WT) or mutant VLP fraction was added and allowed to incubate for 15 min. Reactions were processed for PCR as described in Materials and Methods. PCR was then performed with primers specific to the Ty3 and the *SNR6* target, primers 411 and 242, respectively, using DNA from the integration reactions as the template. PCR products were resolved by electrophoresis on a nondenaturing 8% polyacrylamide gel and visualized by staining with ethidium bromide. The positive control (Pos) was amplified using 5 pg of pDLC370 (for r-U6) and 5 pg of pLY1842 (for l-U6), and the negative control (Neg) lacked VLPs but was otherwise a complete reaction. The sizes of the r-U6 (442 bp) and l-U6 (492 bp) products are shown inside triangles associated with those positions.

number plasmids. These VLPs contained correctly processed capsid, reverse transcriptase, and IN and full-length, 3′-end-processed cDNA (39; data not shown). Recombinant TFIIIB was incubated with *SNR6* target plasmid pLY1855 followed by either wild-type or 419A(3) mutant VLPs as described in Materials and Methods. It has previously been shown that VLPs, a U6 DNA target, and recombinant TFIIIB are sufficient for in vitro integration in the buffer used (see Materials and Methods). After termination of the reaction, DNA was extracted and used as the template for PCR primed by oligonucleotides 411 and 242, which anneal within Ty3 and *SNR6*, respectively. Products were analyzed by nondenaturing polyacrylamide gel electrophoresis.

In the presence of TFIIIB, products representing insertions into the left and right transcription initiation sites of the *SNR6* TATA were apparent for the wild-type Ty3 VLP preparation (Fig. 4, WT). No integration products were observed for the mutant VLPs, even in a reaction with twice the amount of VLPs that resulted in detectable levels of product with wild-type VLPs (Fig. 4, 419, lanes marked 5, 10 μg). Recovery of DNA from the integration reaction was monitored by amplification of the gene for beta-lactamase.

Ty3 IN-GFP fusion proteins localize to yeast nucleolus. A curious aspect of our results with IN (Fig. 1) and IN-GFP (Fig. 2) was that localization corresponded to a poorly staining portion of the region defined by DAPI as the nucleus. The rDNA repeats in yeast localize to the nucleolus, which stains relatively poorly with DAPI. This suggested that Ty3 IN was localized to the nucleolus or an associated structure. A double-staining experiment was performed in which Ty3 IN was visualized as described above using affinity-purified rabbit IgG and secondary goat anti-rabbit IgG antibodies conjugated to Alexa 488 and a nucleolar protein and localized using primary mouse monoclonal antibody YN2C1 (M. Oakes and M. Nomura, personal communication) followed by Alexa 586-conjugated goat anti-mouse IgG antibodies. Alexa 488 and 586 appeared to colocalize to a crescent-shaped compartment of the nucleus, although the staining for IN was extremely weak and more diffuse than for the nucleolar marker (Fig. 1).

The pattern of Ty3 IN-GFP localization was also determined in cells expressing IN-GFP under the *MET25* promoter, which produced a fainter signal representing a lower level of expression. The patterns in cells expressing Nop8p, a known nucleolar protein, fused to GFP or GFP alone, each under control of the *MET25* promoter, were used for comparison with the IN-GFP pattern (54). Expression was induced by growth in medium deficient in methionine. Wild-type IN-GFP expressed under the *MET25* promoter on a centromeric plasmid showed more broadly distributed fluorescence than GFP-NOP8, but the fluorescence was clearly concentrated over a region similar to that stained by GFP-NOP8 (Fig. 5A). Thus, the subnuclear concentration of Ty3 IN-GFP was not unique to cells expressing IN-GFP under the P_{GAL1} promoter and was similar to localization of a known nucleolar protein.

If Ty3 IN-GFP is physically associated with the nucleolus, then cells in which the nucleolus is fragmented should have a similar pattern of staining for IN-GFP. The mutant yeast strain NOY770, a derivative of W303-1a in which a deletion of the rDNA repeat is complemented by a high-copy-number plasmid

containing one copy of the rDNA, has a fragmented nucleolus (40). Therefore, if Ty3 IN-GFP localizes to the nucleolus, it should show a disrupted pattern in this strain. The UAS_{GAL1} Ty3 IN-GFP construct pSSL2050 was transformed into wild-type W303-1a and into NOY770. Cells were induced for Ty3 expression as described above. In the wild-type strain, as previously observed, IN-GFP localized to an apparent subcompartment of the nucleus (Fig. 5B). NOY770 cells were observed in which multiple IN-GFP foci occurred. These corresponded to sites that were poorly staining and located on the periphery of the DAPI-stained region. Similar patterns are observed using nucleolar proteins in this strain (40). Although the presumptive nucleoli in wild-type cells sometimes had tails of IN-GFP fluorescence, multiple foci were not observed. This result was consistent with the interpretation that IN localizes to nucleolar fragments in mutant cells and nucleoli in wild-type cells. In dividing cells, IN-GFP localized to a stripe which corresponded to a subcompartment of the DAPI-stained region.

Ty3 LTRs do not colocalize with rDNA repeats. Cells expressing Ty3 and stained with antibodies to Ty3 IN show fluorescence associated with clustered element proteins in the cytoplasm, but no definitive nuclear signal. Inability to detect nuclear Ty3 proteins complicates evaluation of the physiological implications of nucleolar localization of Ty3 IN. Nevertheless, nucleolar localization has not been reported for retroviral or Ty1 IN proteins. These proteins have not only a similar central domain containing the residues in the catalytic site but similar strand transfer activities as well. This suggests that nucleolar localization of Ty3 is not a nonspecific property associated with DNA binding or strand transfer activities of integrases generally. If nucleolar localization of Ty3 is physiological, then it might be associated with another property that distinguishes Ty3 IN activity from those of other IN proteins—position specificity. The most straightforward rationalization of Ty3 localization to the nucleolus, if it occurs, would be that Ty3 integration targets are concentrated in that part of the nucleus. A study that selected strains with insertions expressing a *HIS3* marker in Ty3 recovered 91 elements, of which all sequenced copies were associated with tRNA genes (9), suggesting that the predominant genomic target of Ty3 integration is tRNA genes. Several reports have recently raised the intriguing possibility that at least a subset of these genes may be associated with the nucleolus (3, 51).

In order to explore the possibility that tRNA gene targets of Ty3 integration are associated with the nucleolus, we undertook an experiment to test the colocalization of Ty3 sequences with rDNA. Because Ty3 and its approximately 40 340-bp LTRs are associated virtually exclusively with tRNA genes, these sequences provide an excellent probe for the nuclear positions of approximately one seventh of the 272 genomic tRNA genes (17). FISH analysis was undertaken to localize Ty3 insertion sites relative to the rDNA (Fig. 6). An rDNA probe was biotinylated using random priming in order to visualize the nucleolus. Cells were stained with rDNA and also with control plasmid, Ty3 LTR, or Ty3 probe. The non-rDNA probes were labeled with digoxigenin, using random priming and digoxigenin-11-UTP. Hybridized biotinylated (rDNA) probes were visualized with FITC-avidin, biotinylated antiavidin, and FITC-avidin. Hybridized digoxigenin (pUC, LTR, and
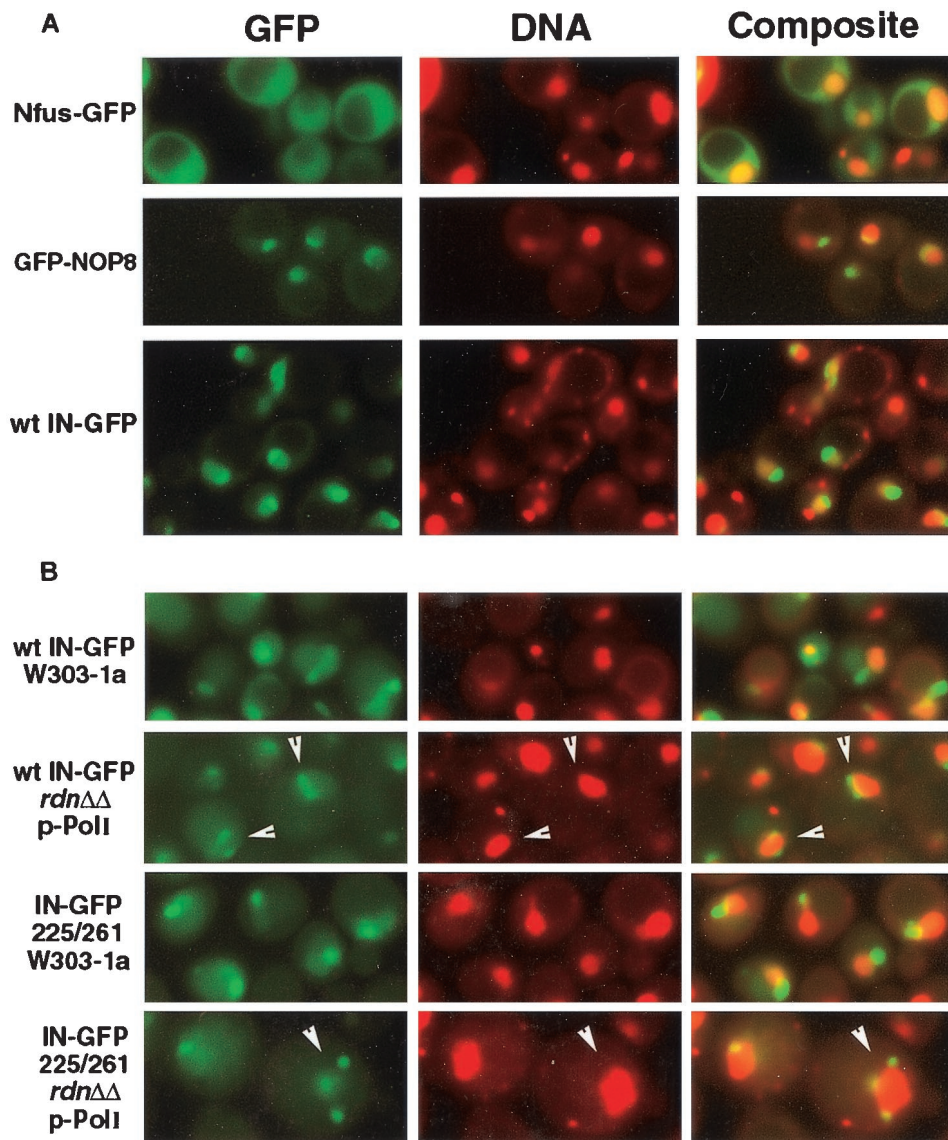
FIG. 5. (A) Similar localization of IN-GFP and a nucleolar protein fused to GFP. Yeast cells expressing GFP, GFP-NOP8, and wild-type (wt) Ty3 IN-GFP under P_{MET25} were analyzed for fusion protein and DNA localization. Images of GFP and DNA were pseudocolored green and red, respectively. Individual images were overlaid, and regions of colocalization appear as orange to yellow fluorescence. (B) Fragmentation of Ty3 IN-GFP localization in rDNA deletion mutants with fragmented nucleoli. Ty3 IN-GFP and D225E/E261D IN-GFP were expressed in yeast strain W303-1a and its derivative, NOY770. In this mutant, which lacks chromosomal rDNA and expresses rRNA from a high-copy-number plasmid, the nucleolus is fragmented. White arrowheads indicate examples of cells with nucleolar fragments. GFP and DNA are visualized as described for Fig. 2.

Ty3) probes were detected using mouse antidigoxigenin IgG followed by anti-mouse IgG–Alexa 586. DNA was visualized by DAPI staining.

Hybridization showed that the rDNA, as expected, was localized to a crescent along one side of the nucleus. The control probe showed reactivity over the cells but was not localized to any particular structure (Fig. 6, top row). The Ty3 LTR probe hybridized to multiple sites per nucleus but did not concentrate with rDNA staining (second row). The Ty3 probe, which included one copy of the LTR, stained more brightly than the LTR-specific probe, but also did not localize within the region stained by the rDNA probe (third row). Our experiments do not exclude the possibility that a subset of tRNA genes are

localized to the nucleolus. In addition, it is formally possible that tRNA genes identified with these probes were nucleolar at the time of Ty3 insertion. Nevertheless, these results did not support the hypothesis that Ty3 targets are restricted to the nucleolus.

Ty3 can use genomic 5S rRNA genes as its transposition targets. In addition to tRNA genes, Ty3 targets other genes transcribed by RNA polymerase III, including the 5S genes. In yeast, the approximately 120 copies of 5S rDNA are within the rDNA repeat. Thus, if Ty3 targeted genomic 5S rDNAs, nucleolar localization could play a role in targeting. The 5S genes have been shown to act as plasmid targets for Ty3 integration, used at about one-fourth the frequency that tRNA genes are
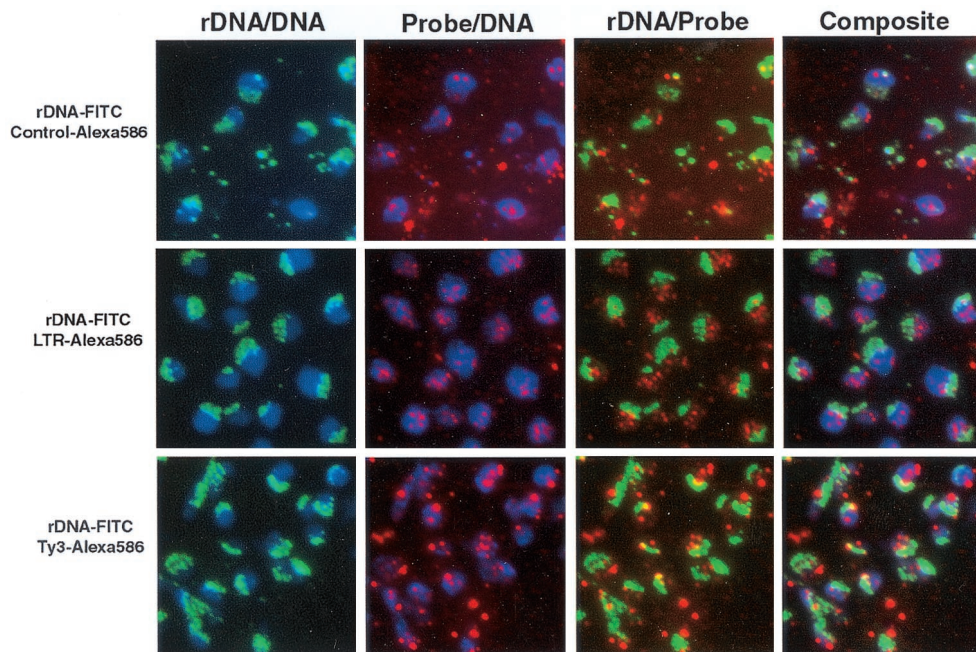
FIG. 6. LTR, Ty3, and rDNA sequences do not all localize to the nucleolus. W303-1a cells were analyzed for the nuclear location of the genomic LTR and Ty3 sequences compared to rDNA. Probes containing rDNA sequences were biotinylated and detected by successive incubations in FITC-avidin, biotinylated antiavidin, and finally FITC-avidin (pseudocolored green). Probes containing control plasmid, LTR, or Ty3 sequences were labeled with digoxigenin. Hybridized digoxigenin probes were detected using antidigoxigenin and then anti-mouse IgG-Alexa-586 (pseudocolored red). DNA was stained with DAPI (pseudocolored blue). Each frame represents the indicated overlay.

used (10). However, to date there is no evidence for their use as genomic targets. In the study of 91 genomic insertions of the *HIS3*-marked Ty3, assuming their less efficient use compared to tRNA genes, at least 1/10 of the insertions should have been into 5S rDNAs. Southern blot analysis was used to specifically probe for insertions into the 5S rDNAs in HIS^+ cells. However, no cells containing Ty3 genomic insertions were identified. Chromosomal rDNA in yeast is repressed for recombination (18) and expression of genes transcribed by RNA polymerase II (6, 49). Thus, failure to recover Ty3 insertions in the rDNA could be attributed to either interference with integration, so that chromosomal 5S genes are prevented from acting as targets, or to failure to select cells with insertions expressing the Ty3 *HIS3* marker under conditions of the assay.

To circumvent the requirement of the genetic assay for marker expression, a PCR assay was developed for detection of insertions into the rDNA locus. This assay was similar to previous PCR assays for Ty3 integration but relied on a combination of primers that annealed in the Ty3 and in the 5S genes. Control experiments used a 5S plasmid that contains a Ty3 insertion isolated during an in vivo transposition study (D. Chalker and S. B. Sandmeyer, unpublished results) (Fig. 7, lanes P). Yeast strain yTM443 was transformed with low-copy-number plasmid pMA1833 or pMA1890, expressing *GAL1*-regulated wild-type and IN(D255E/E261D) Ty3, respectively. Twelve isolates of each were inoculated into 9 ml of SR-Ura and grown overnight at 30°C to log phase (OD_{600} of 0.3 to 0.4). Transcription of Ty3 was induced by addition of galactose to 2%, and cells were incubated for 6 h. The cells were harvested, and genomic DNA was extracted, purified, and quantified. PCR was performed using 125 ng of genomic template DNA

together with primers 411 and 720, which anneal in Ty3 and the 5S rDNA sequence, respectively. PCR products were resolved by electrophoresis on a nondenaturing polyacrylamide gel and visualized by staining with ethidium bromide.
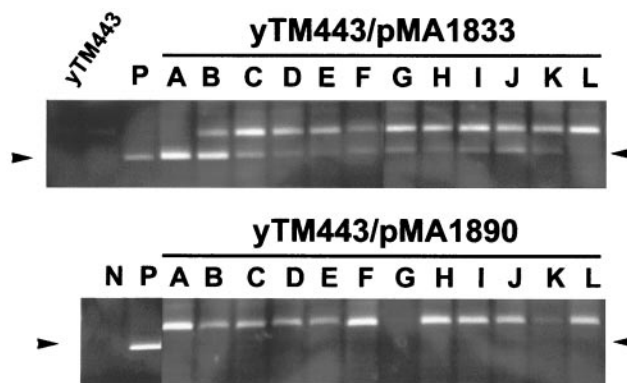

FIG. 7. Detection of 5S integration using PCR. Top panel, yTM443 transformed with a low-copy-number plasmid expressing wild-type Ty3 (pMA1833) (upper panel) or Ty3 IN catalytic mutant (pMA1890) (lower panel) was induced for transposition in the presence of galactose for 6 h, and the DNA was harvested for PCR analysis. Ty3 elements integrated into the 5S rDNA were amplified using primers 411 (Ty3) and 720 (5S rDNA), and the PCR products were resolved by electrophoresis on a nondenaturing polyacrylamide gel and visualized by staining with ethidium bromide. Arrows indicate the positions of the amplified integration fragment. Negative control (N) contains only genomic DNA and primers. Positive control (P) contains genomic DNA, primers, and 0.05 ng of pDLC322, a plasmid containing a Ty3 upstream of a 5S rDNA gene (D. Chalker, unpublished data).

Most reactions using genomic DNA templates from cells expressing wild-type Ty3 showed a fragment of the same size as the positive-control fragment, although the intensity of this fragment varied considerably (Fig. 7, lanes A to L, upper panel). Reactions templated by genomic DNA from cells expressing IN(D255E/E261D) did not produce this fragment (Fig. 7, lanes A to L, lower panel). Thus, Ty3 insertions into genomic 5S genes do occur, although it is not yet possible to compare the global frequency for 5S genes to that for tRNA genes because of the PCR background problems created by existing LTRs associated with most families of tRNA genes (data not shown).

DISCUSSION

Identification of the NLS for Ty3 provides an entrée to understanding regulation of a key step in the life cycle of this retrotransposon. Nuclear entry is of particular interest, as the analogous step in the case of animal retroviruses appears to distinguish viruses that can infect nondividing cells from those which cannot. Additional interest arises from the observation that even for infection of dividing cells, the NLS motif may be essential for some retroviruses. In the current investigation, IN was shown to be capable of targeting itself, as well as an IN-GFP fusion, to the nucleus. It was previously shown that mutations in Ty3 affecting charged IN residues in the vicinity of aa 412 and 419 block Ty3 transposition but do not disrupt 3′-end processing. These residues are localized to a bipartite basic region contained within aa 401 to 436 that is sufficient to target a covalent dimer of GFP to the nucleus. Thus, the NLS of Ty3 is located in the carboxyl-terminal domain of IN, similar to positions of HIV-1, ASV, and Ty1 NLS motifs in their respective IN proteins.

The Ty3 NLS is distinct from the NLS motif of the other gypsylike element, Tf1. That NLS is a monopartite basic domain located within the major structural protein (13). While it is presumed that the earliest-acting defect in these mutants is the block in nuclear entry, this could not be assessed directly because nuclear entry of IN in cells expressing Ty3 was not detectable using Ty3 IN antiserum (data not shown). Identification of the Ty3 NLS extends the members of the retroelement class, including retroviruses, with bipartite or extended regions containing basic residues with NLS activity. These include HIV-1 IN (16), Ty1 IN (27, 36), and ASV (30). The finding that NLS mutant Ty3 VLPs are not active in strand transfer in vitro suggests that, similar to the HIV NLS, these residues may have functions in addition to nuclear entry.

A blast search of the Ty3 NLS motif using the *Saccharomyces* Genome Database (http://genome-www.stanford.edu/Saccharomyces/) did not reveal any non-Ty3 identical matches with the Ty3 motif. Short sequences within the domain did show similarity to other proteins (data not shown), but the significance of these was not compelling. A large number of gypsylike elements have now been identified, and the IN proteins have been compared. The NLS peptide domain identified here for Ty3 lies carboxyl-terminal to the conserved central region of these IN proteins and overlaps the carboxyl-terminal portion of a block of residues conserved among a set of gypsylike elements which is referred to as the GPY/F domain (34). The pattern of basic residues found in this portion of Ty3 does not appear to be highly conserved among gypsylike elements, although other elements do have concentrations of basic residues in the vicinity (data not shown). Interestingly, this is just amino-terminal of the chromodomain that occurs in some gypsylike elements but not in Ty3 (34).

This study did not directly address the pathway through which Ty3 enters the nucleus. Other bipartite NLS signals in yeast, for example, nucleoplasmin (14), have been shown to interact with importin α. Localization of overexpressed, ectopic Ty3 IN to a subcompartment of the nucleus, the nucleolus, was observed. At least some nucleolar proteins appear to enter the nucleus through importin α-independent pathways mediated by importin β homologs (52). However, until preintegration complexes are visualized in the nuclei of cells expressing intact Ty3, it is a matter of speculation whether Ty3 preintegration complexes are similarly targeted. In contrast to NLS motifs, nucleolar localization signals (NOS) are not well defined. Some NOS are contiguous with the NLS, and some are discrete (47). Some defined NOS consist of extended basic regions or RG repeats, neither of which is obvious in the Ty3 IN sequence. Because the NLS peptide did not localize the GFP fusion to the nucleolus, the Ty3 IN NOS must encompass additional residues or be separated from the NLS. Interestingly, Ty3 transposition is sensitive to overexpression of a number of proteins involved in translation, including particular ribosomal proteins (J. Claypool and S. B. Sandmeyer, unpublished data). Whether this could be related to competition with nuclear transport is not yet known.

Ty3 is position specific for genes transcribed by polymerase III. It is intriguing to consider that nucleolar localization of the Ty3 preintegration complex, if it occurs, could contribute to delivery of Ty3 DNA to genomic targets. Previous studies have indicated that pre-tRNAs and processing complexes may be distributed between nucleolar and nonnucleolar loci (25, 45). However, electron microscopic localization of a polymerase III subunit in *S. cerevisiae* failed to find a significant concentration of the protein in the nucleolus, suggesting that the majority of polymerase III is not nucleolar (32). In this study we also did not find evidence that tRNA genes, the previously identified major chromosomal target of Ty3 integration, are generally localized to the nucleolus. However, Ty3 also targets 5S genes, which are presumed to be nucleolar by virtue of their association with the rDNA in yeast. In this study, we found that integration at sites adjacent to 5S chromosomal genes could be detected using PCR, a physical method, rather than genetic selection. Thus, nucleolar targeting could contribute to insertions at a subset of polymerase III-transcribed genes.

A mutation involving IN residues 419 to 421 within the NLS blocked in vitro integration mediated by Ty3 VLPs. The stringency of ordering of DNA replication relative to nuclear entry and nuclear entry relative to DNA 3-end processing for retroviruses and retroviruslike elements is not clear. The Ty3 mutation NLS mutation did not block 3-end processing (39). Thus, 3-end processing is not dependent on nuclear entry. Nevertheless, in the in vitro assay, fractions containing particles from cells expressing the mutant NLS failed to show significant amounts of integration at a tRNA gene target. This result appears to distinguish Ty3 nuclear localization mutants from Ty1 nuclear localization mutants which have been reported to have integration activity in vitro (27, 36). However,

the conditions of the respective assays were not identical, making it difficult to conclude that this necessarily represents a significant biological difference between the two types of elements.

It is presumed that retroviruses and retrotransposons must undergo uncoating to negotiate the nuclear pore. IN contains the NLS and, in models proposed for retroviral structure, would be presumed to be internal, making exposure of the NLS secondary to uncoating. Nevertheless, the signals for uncoating are not known, and post-reverse transcription, IN might play a role in this process. Alternatively, passage through the nuclear pore could be essential for activation of the preintegration complex in some way. A simpler scenario is suggested by the proximity of the NLS and presumed DNA-binding domains of IN. The basic NLS and DNA-binding domains of other proteins have been found to overlap. Indeed, this overlapping function has been suggested as the explanation for the failure of HIV-1 NLS mutants to integrate in dividing host cells (data not shown) (16).

In summary, the current study identified a motif in the Ty3 IN that is essential and sufficient for nuclear localization. Mutations in this domain blocked integration in vitro, suggesting a dual function for the NLS motif. In addition, our study raises the intriguing possibility that nucleolar localization of retroelements could occur and contribute to insertion specificity for at least a subset of sites.

ACKNOWLEDGMENTS

REFERENCES

1. **Atwood, A., J. H. Lin, and H. L. Levin.** 1996. The retrotransposon Tf1 assembles virus-like particles that contain excess Gag relative to integrase because of a regulated degradation process. Mol. Cell. Biol. **16:**338–346.
2. **Ausubel, F. M., R. Brent, R. E. Kingston, D. D. Moore, J. G. Seidman, J. A. Smith, and K. Struhl.** 1998. Current protocols in molecular biology. Greene Publishing Associates/Wiley-Interscience, New York, N.Y.
3. **Bertrand, E., F. Houser-Scott, A. Kendall, R. H. Singer, and D. R. Engelke.** 1998. Nucleolar localization of early tRNA processing. Genes Dev. **12:**2463–2468.
4. **Bilanchone, V. W., J. A. Claypool, P. T. Kinsey, and S. B. Sandmeyer.** 1993. Positive and negative regulatory elements control expression of the yeast retrotransposon Ty3. Genetics **134:**685–700.
5. **Boeke, J. D. and J. P. Stoye.** 1997. Retrotransposons, endogenous retroviruses, and the evolution of retroelements, p. 343–435. *In* J. M. Coffin, S. H. Hughes, and H. E. Varmus (ed.), Retroviruses. Cold Spring Harbor Press, Cold Spring Harbor, N.Y.
6. **Bryk, M., M. Banerjee, M. Murphy, K. E. Knudsen, D. J. Garfinkel, and M. J. Curcio.** 1997. Transcriptional silencing of Ty1 elements in the *RDN1* locus of yeast. Genes Dev. **11:**255–269.
7. **Bukrinsky, M. I., and O. K. Haffar.** 1999. HIV-1 nuclear import: in search of a leader. Front. Biosci. **4:**D772–D781.
8. **Castano, I. B., P. M. Brzoska, B. U. Sadoff, H. Chen, and M. F. Christman.** 1996. Mitotic chromosome condensation in the rDNA requires TRF4 and DNA topoisomerase I in *Saccharomyces cerevisiae*. Genes Dev. **10:**2564–2576.
9. **Chalker, D. L., and S. B. Sandmeyer.** 1990. Transfer RNA genes are genomic targets for *de novo* transposition of the yeast retrotransposon Ty3. Genetics **126:**837–850.
10. **Chalker, D. L., and S. B. Sandmeyer.** 1992. Ty3 integrates within the region of RNA polymerase III transcription initiation. Genes Dev. **6:**117–128.
11. **Chernoff, Y. O., A. Vincent, and S. W. Liebman.** 1994. Mutations in eukaryotic 18S ribosomal RNA affect translational fidelity and resistance to ami-

noglycoside antibiotics. EMBO J. **13:**906–913.
12. **Corbett, A. H., and P. A. Silver.** 1997. Nucleocytoplasmic transport of macromolecules. Microbiol. Mol. Biol. Rev. **61:**193–211.
13. **Dang, V. D., and H. L. Levin.** 2000. Nuclear import of the retrotransposon Tf1 is governed by a nuclear localization signal that possesses a unique requirement for the FXFG nuclear pore factor nup124p. Mol. Cell. Biol. **20:**7798–7812.
14. **Fabre, E., and E. Hurt.** 1997. Yeast genetics to dissect the nuclear pore complex and nucleocytoplasmic trafficking. Annu. Rev. Genet. **31:**277–313.
15. **Fouchier, R. A., and M. H. Malim.** 1999. Nuclear import of human immunodeficiency virus type-1 preintegration complexes. Adv. Virus Res. **52:**275–299.
16. **Gallay, P., T. Hope, D. Chin, and D. Trono.** 1997. HIV-1 infection of non-dividing cells through the recognition of integrase by the importin/karyopherin pathway. Proc. Natl. Acad. Sci. USA **94:**9825–9830.
17. **Goffeau, A., B. G. Barrell, H. Bussey, R. W. Davis, B. Dujon, H. Feldmann, J. D. Hoheisel, C. Jacq, M. Johnston, E. J. Louis, H. W. Mewes, Y. Murakkmi, P. Philippsen, H. Tettelin, and S. G. Oliver.** 1996. Life with 6000 genes. Science **274:**546–567.
18. **Gottlieb, S., and R. E. Esposito.** 1989. A new role for a yeast transcriptional silencer gene, *SIR2*, in regulation of recombination in ribosomal DNA. Cell **56:**771–776.
19. **Guacci, V., E. Hogan, and D. Koshland.** 1994. Chromosome condensation and sister chromatid pairing in budding yeast. J. Cell Biol. **125:**517–530.
20. **Hansen, L. J., D. L. Chalker, K. J. Orlinsky, and S. B. Sandmeyer.** 1992. Ty3 *GAG3* and *POL3* genes encode the components of intracellular particles. J. Virol. **66:**1414–1424.
21. **Hansen, L. J., D. L. Chalker, and S. B. Sandmeyer.** 1988. Ty3, a yeast retrotransposon associated with tRNA genes, has homology to animal retroviruses. Mol. Cell. Biol. **8:**5245–5256.
22. **Hansen, L. J., and S. B. Sandmeyer.** 1990. Characterization of a transpositionally active Ty3 element and identification of the Ty3 integrase protein. J. Virol. **64:**2599–2607.
23. **Heim, R., A. B. Cubitt, and R. Y. Tsien.** 1995. Improved green fluorescence. Nature **373:**663–664.
24. **Heinzinger, N. K., M. I. Bukrinsky, S. A. Haggerty, A. M. Ragland, V. Kewalramani, M. A. Lee, H. E. Gendelman, L. Ratner, M. Stevenson, and M. Emerman.** 1994. The Vpr protein of human immunodeficiency virus type 1 influences nuclear localization of viral nucleic acids in nondividing host cells. Proc. Natl. Acad. Sci. USA **91:**7311–7315.
25. **Hull, M. W., J. Erickson, M. Johnston, and D. R. Engelke.** 1994. tRNA genes as transcriptional repressor elements. Mol. Cell. Biol. **14:**1266–1277.
26. **Kalderon, D., W. D. Richardson, A. F. Markham, and A. E. Smith.** 1984. Sequence requirements for nuclear location of simian virus 40 large-T antigen. Nature **311:**33–38.
27. **Kenna, M. A., C. Baker Brachmann, S. E. Devine, and J. D. Boeke.** 1998. Invading the yeast nucleus: a nuclear localization signal at the C terminus of Ty1 integrase is required for transposition in vivo. Mol. Cell. Biol. **18:**1115–1124.
28. **Kinsey, P., and S. Sandmeyer.** 1995. Ty3 transposes in mating populations of yeast: a novel transposition assay for Ty3. Genetics **139:**81–94.
29. **Kirchner, J., and S. B. Sandmeyer.** 1996. Ty3 integrase mutants defective in reverse transcription or 3′ end processing of extrachromosomal Ty3 DNA. J. Virol. **70:**4737–4747.
30. **Kukolj, G., R. A. Katz, and A. M. Skalka.** 1998. Characterization of the nuclear localization signal in the avian sarcoma virus integrase. Gene **223:**157–163.
31. **Kunkel, T. A.** 1985. Rapid and efficient site-specific mutagenesis without phenotypic selection. Proc. Natl. Acad. Sci. USA **82:**488–492.
32. **Leger-Silvestre, I., S. Trumtel, J. Noaillac-Depeyre, and N. Gas.** 1999. Functional compartmentalization of the nucleus in the budding yeast *Saccharomyces cerevisiae*. Chromosoma **108:**103–113.
33. **Mahalingam, S., S. A. Khan, M. A. Jabbar, C. E. Monken, R. G. Collman, and A. Srinivasan.** 1995. Identification of residues in the N-terminal acidic domain of HIV-1 Vpr essential for virion incorporation. Virology **207:**297–302.
34. **Malik, H. S., and T. H. Eickbush.** 1999. Modular evolution of the integrase domain in the Ty3/gypsy class of LTR retrotransposons. J. Virol. **73:**5186–5190.
35. **Menees, T. M., and S. B. Sandmeyer.** 1994. Transposition of the yeast retroviruslike element Ty3 is dependent on the cell cycle. Mol. Cell. Biol. **14:**8229–8240.
36. **Moore, S. P., L. A. Rinckel, and D. J. Garfinkel.** 1998. A Ty1 integrase nuclear localization signal required for retrotransposition. Mol. Cell. Biol. **18:**1105–1114.
37. **Mumberg, D., R. Muller, and M. Funk.** 1995. Yeast vectors for the controlled expression of heterologous proteins in different genetic backgrounds. Gene **156:**119–122.
38. **Nakai, K., and M. Kanehisa.** 1992. A knowledge base for predicting protein localization sites in eukaryotic cells. Genomics **14:**897–911.
39. **Nymark-McMahon, M. H., and S. B. Sandmeyer.** 1999. Mutations in non-

conserved domains of Ty3 integrase affect multiple stages of the Ty3 life cycle. J. Virol. **73:**453–465.

40. **Oakes, M., J. P. Aris, J. S. Brockenbrough, H. Wai, L. Vu, and M. Nomura.** 1998. Mutational analysis of the structure and localization of the nucleolus in the yeast *Saccharomyces cerevisiae*. J. Cell Biol. **143:**23–34.

41. **Oakes, M., Y. Nogi, M. W. Clark, and M. Nomura.** 1993. Structural alterations of the nucleolus in mutants of *Saccharomyces cerevisiae* defective in RNA polymerase I. Mol. Cell. Biol. **13:**2441–2455.

42. **Pluymers, W., P. Cherepanov, D. Schols, E. De Clercq, and Z. Debyser.** 1999. Nuclear localization of human immunodeficiency virus type 1 integrase expressed as a fusion protein with green fluorescent protein. Virology **258:**327–332.

43. **Popov, S., M. Rexach, L. Ratner, G. Blobel, and M. Bukrinsky.** 1998. Viral protein R regulates docking of the HIV-1 preintegration complex to the nuclear pore complex. J. Biol. Chem. **273:**13347–13352.

44. **Sandmeyer, S. B., and T. M. Menees.** 1996. Morphogenesis at the retrotransposon-retrovirus interface: Gypsy and Copia families in yeast and *Drosophila*. Curr. Top. Microbiol. Immunol. **214:**261–296.

45. **Sarkar, S., and A. K. Hopper.** 1998. tRNA nuclear export in *Saccharomyces cerevisiae*: in situ hybridization analysis. Mol. Biol. Cell **9:**3041–3055.

46. **Schiestl, R. H., and D. R. Gietz.** 1989. High efficiency transformation of intact yeast cells using single stranded nucleic acids as a carrier. Curr. Genet. **16:**339–346.

47. **Shaw, P. J., and E. G. Jordan.** 1995. The nucleolus. Annu. Rev. Cell Dev. Biol. **11:**93–121.

48. **Sikorski, R. S., and P. Hieter.** 1989. A system of shuttle vectors and yeast host strains designed for efficent manipulation of DNA in *Saccharomyces cerevisiae*. Genetics **122:**19–27.

49. **Smith, J. S., and J. D. Boeke.** 1997. An unusual form of transcriptional silencing in yeast ribosomal DNA. Genes Dev. **11:**241–254.

50. **Whittaker, G. R., and A. Helenius.** 1998. Nuclear import and export of viruses and virus genomes. Virology **246:**1–23.

51. **Wolin, S. L., and A. G. Matera.** 1999. The trials and travels of tRNA. Genes Dev. **13:**1–10.

52. **Wozniak, R. W., M. P. Rout, and J. D. Aitchison.** 1998. Karyopherins and kissing cousins. Trends Cell Biol. **8:**184–188.

53. **Yieh, L., G. Kassavetis, E. P. Geiduschek, and S. B. Sandmeyer.** 2000. The brf and TATA-binding protein subunits of the RNA polymerase III transcription factor IIIB mediate position-specific integration of the gypsy-like element, Ty3. J. Biol. Chem. **275:**29800–29807.

54. **Zanchin, N. I., and D. S. Goldfarb.** 1999. Nip7p interacts with Nop8p, an essential nucleolar protein required for 60S ribosome biogenesis, and the exosome subunit Rrp43p. Mol. Cell. Biol. **19:**1518–1525.

55. **Zennou, V., C. Petit, D. Guetard, U. Nerhbass, L. Montagnier, and P. Charneau.** 2000. HIV-1 genome nuclear import is mediated by a central DNA flap. Cell **101:**173–185.